

Intersubband phonon overlap integrals for AlGaAs/GaAs single-well heterostructures

Kiyoyuki Yokoyama and Karl Hess

*Coordinated Science Laboratory, University of Illinois at Urbana-Champaign,
Urbana, Illinois 61801*

(Received 1 March 1985)

The five lowest subband coupling coefficients $H_{mn}(Q)$ are calculated for polar-optical-phonon scattering in $\text{Al}_{0.3}\text{Ga}_{0.7}\text{As}/\text{GaAs}$ single-well heterostructures. The wave functions are calculated self-consistently within the effective-mass approximation including exchange and correlation effects.

Much effort has been made to advance the understanding of the electronic transport properties of quasi-two-dimensional systems.¹ Following the pioneering studies of Stern and Howard for inversion layers of metal-oxide semiconductor field-effect transistors (MOSFET's),² Ando performed detailed studies of MOSFET's and AlGaAs/GaAs single-well structures.³ Simultaneously, lattice scattering for electrons in heterolayers has been extensively studied.⁴⁻⁶ Intraband scattering is well understood. Intersubband scattering has been investigated in less detail.⁶ It is the purpose of this Communication to present an accurate calculation of the overlap integrals which are necessary to determine intersubband scattering by phonons. The two-dimensional carrier scattering rate between m th and n th subbands is proportional to⁵

$$|M_{mn}|^2 = \int |Q, q|^2 |I_{mn}(q)|^2 dq, \quad (1)$$

where $M(Q, q)$ is the corresponding three-dimensional matrix element, and Q and q are phonon-wave-vector components parallel (xy plane) and normal (z direction) to the layer interfaces, respectively. The overlap integral is expressed as⁵

$$I_{mn}(q) = \int F_m(z) F_n(z) \exp(iqz) dz, \quad (2)$$

where $F_m(z)$ is the normalized envelope function corresponding to the quantized energy of E_m .

Polar-optical-phonon scattering is one of the dominant scattering mechanisms above 77 K in III-V compound semiconductors. For polar-optical-phonon scattering, $|M(Q, q)|^2$ is proportional to $1/(Q^2 + q^2)$. Accordingly, the scattering rate is proportional to $H_{mn}(Q)/Q$, where the multiband coupling coefficients are expressed as⁶

$$H_{mn}(Q) = \int \int dz_1 dz_2 F_{mn}(z_1) F_{mn}(z_2) \exp(-Q|z_1 - z_2|). \quad (3)$$

Here $F_{mn}(z) = F_m(z) F_n(z)$.

Since most of the electrons populate the lowest subband at low temperatures, the value of $H_{11}(Q)$ has been worked out in detail.⁷ However, the electron occupation probability of higher subbands increases in high electric fields (the electrons become hot), and both intrasubband scattering in higher subbands and intersubband scattering among higher subbands are no longer negligible, even at a lattice temperature of 77 K. Under these conditions, the knowledge of the coefficients $H_{mn}(Q)$ is necessary in order to accurately calculate the optical phonon scattering rates for each subband. Self-consistent numerical calculations provide not only the

quantized energy levels (E_m) but also the corresponding wave functions $[F_m(z)]$ for a realistic AlGaAs/GaAs single-well heterostructure. Using these wave functions, accurate values of $H_{mn}(Q)$ can be obtained. The self-consistent calculation is briefly described in the following.

The normalized wave-function $F_m(z)$ for the m th subband can be obtained from the Schrödinger equation

$$-\frac{\hbar^2}{2m^*} \frac{d^2 F_m(z)}{dz^2} + V(z) F_m(z) = E_m F_m(z). \quad (4)$$

The effective potential $V(z)$ is given by

$$V(z) = -e\phi(z) + V_h(z) + V_{xc}(z), \quad (5)$$

where $\phi(z)$ is the electrostatic potential given by the solution of Eq. (6) below, $V_h(z)$ is the step function describing the interface barrier, and $V_{xc}(z)$ is the local exchange correlation potential.⁸ We take into account the five lowest subbands. Then, Poisson's equation reads

$$\frac{d^2 \phi(z)}{dz^2} = \frac{e}{\epsilon_0 \epsilon} \left(\sum_{i=1}^5 N_i F_i^2(z) + N_A(z) - N_D(z) \right), \quad (6)$$

where N_i represents the number of electrons in subband i and is given by

$$N_i = \frac{m^* k_B T}{\pi \hbar^2} \ln \left[1 + \exp \left(\frac{E_F - E_i}{k_B T} \right) \right]. \quad (7)$$

$N_A(z)$ and $N_D(z)$ are the position-dependent acceptor and donor concentrations, and E_F is the Fermi energy.

In the calculation, we used an effective mass $m^* = 0.067m_0$ and a dielectric constant $\epsilon = 13.0$ uniformly in both GaAs and AlGaAs. We have assumed abrupt interfaces, a barrier height of 0.3 eV, and we have neglected the image force term in Eq. (5). All of these approximations are very reasonable according to the results reported by Stern.⁹ Moreover, the mobile charge in the AlGaAs layer was assumed to be depleted except for the penetration of the wave function of electrons from GaAs into AlGaAs. To solve the Schrödinger equation, we used the Numerov method,¹⁰ which is efficient to obtain the pairs of eigenvalues and eigenfunctions accurately within short computational times.

Figure 1 shows the calculated effect potential according to Eq. (5) together with the five lowest subband energy levels at 77 K. The broken line indicates the electron concentration which is derived from the first term in the right parentheses of Eq. (6). The structure parameters are shown in the figure caption. The calculated energy differences

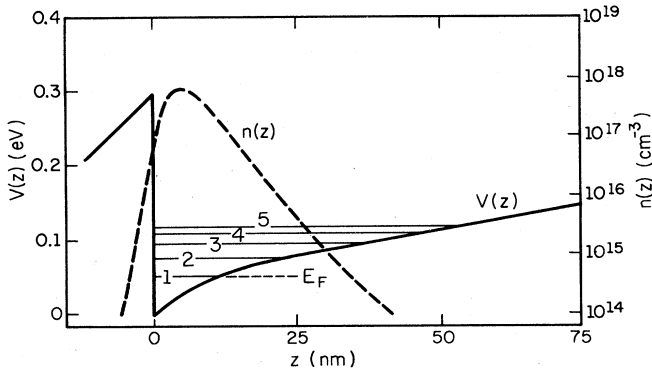


FIG. 1. Calculated effective potential $V(z)$ defined by Eq. (5) and electron distribution $n(z)$ at 77 K. In this calculation, $5 \times 10^{11} \text{ cm}^{-2}$ electrons in GaAs channel (N_s), an acceptor doping of $1 \times 10^{15} \text{ cm}^{-3}$ in the GaAs, 40 nm of $\text{Al}_{0.3}\text{Ga}_{0.7}\text{As}$ layer with a donor concentration of $5 \times 10^{17} \text{ cm}^{-3}$, and 10 nm of unintentionally doped $\text{Al}_{0.3}\text{Ga}_{0.7}\text{As}$ spacer were assumed. The heterointerface was chosen to be at $z = 0$ (GaAs layer: $z > 0$). The numbers in the figure indicate the quantized energy levels of the five lowest subbands.

between the nearest two subbands were 28.7, 17.3, 14.0, and 12.3 meV, and the Fermi energy was 0.5 meV below the bottom of the first miniband, as shown in Fig. 1.

Figure 2 shows the calculated multisubband coupling coefficients $H_{mn}(Q)$, together with the envelope functions $F_m(z)$. Considering two limiting cases for Q , very large and small Q values, Price proposed an explicit approximation⁵ which is for intrasubband scattering given by

$$H_{mm}(Q) \approx 1/(1 + b_{mm}Q), \quad (8)$$

where b_{mm} is the effective well width defined by $1/b_{mm} = 2 \int F_m^2(z) dz$. Corresponding to Fig. 1, the obtained effective widths from the first to the fifth subbands were 6.60, 10.98, 14.39, 17.25, and 19.80 nm, respectively. By substituting these values into approximation (8), we have obtained approximate values, which are in good agreement with the more exact numerical results. The agreement is especially good for subbands higher than the second. In the lower subbands, a maximum error occurs at around $Q = 2 \times 10^6 \text{ cm}^{-1}$, and the approximation differs from the exact results for the two lowest subbands by 13.3 and 8.5%.

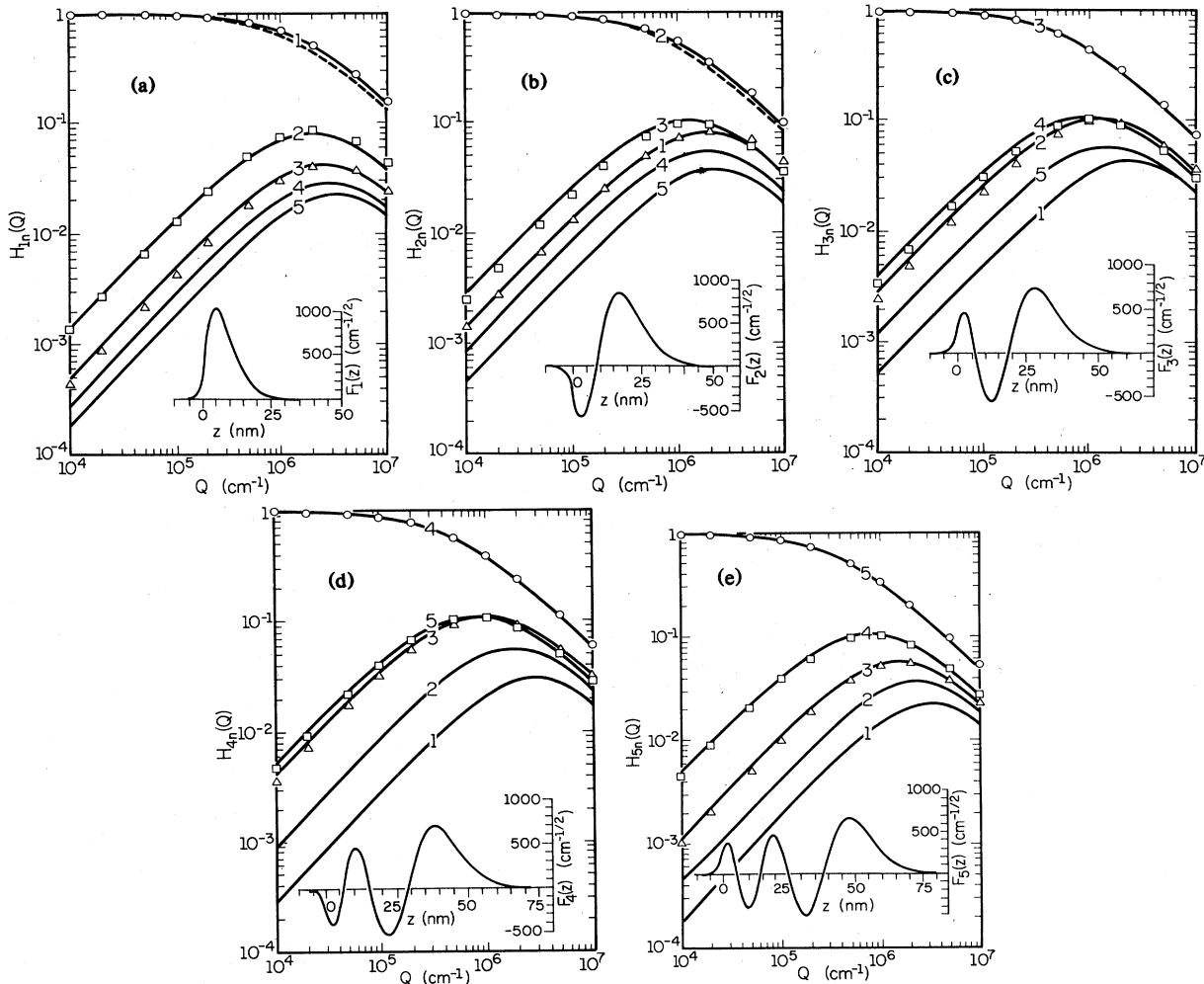


FIG. 2. Calculated multisubband coupling coefficients for (a) first, (b) second, (c) third, (d) fourth, and (e) fifth subbands. Solid lines show the numerical results obtained from Eq. (3). The broken lines in (a) and (b) indicate the approximate results using Eq. (8) and numerically obtained values of b_{11} and b_{22} . Open rectangles, triangles, and circles show the results for the two most important coefficients $H_{11}(Q)$ and $H_{22}(Q)$, respectively, at 300 K. The insertions indicate the corresponding wave functions at 77 K. The material parameters are the same as for Fig. 1.

In Fig. 2, the approximate values are also shown for the lowest two subbands.

Our numerical results show that the values of $H_{mn}(Q)$ are much smaller than those of $H_{mm}(Q)$. Analogous to the intrasubband coupling coefficients, $H_{mn}(Q)$ may be approximated as $C_{mn}Q/(1 + b_{mn}C_{mn}Q^2)$.^{6,11} However, this approximation is rather poor. For example, the approximate value of $H_{12}(2 \times 10^6 \text{ cm}^{-1})$ is 112% larger than that of the exact solution. Consequently, it is necessary to obtain the more exact numerical results for $H_{mn}(Q)$ in order to accurately calculate intersubband phonon scattering. The open rectangles and triangles in Fig. 2 show the two most important coefficients $H_{mn}(Q)$ at 300 K for each of the five subbands. The open circles also indicate the corresponding values of $H_{mm}(Q)$. Although the subband energy levels and the occupation probabilities are very different for the two temperatures of 77 and 300 K (Ref. 12), the curves of $H_{mn}(Q)$ are not. For example, the deviation of $H_{12}(Q)$ is 8.2% at $Q = 2 \times 10^6 \text{ cm}^{-1}$. We have also investigated the dependence of $H_{mn}(Q)$ on the inversion carrier density N_s . Gen-

erally, this dependence is also weak. We found that $H_{12}(2 \times 10^6 \text{ cm}^{-1})$ increases by 22.7% when decreasing N_s from $5 \times 10^{11} \text{ cm}^{-2}$ to $1 \times 10^{11} \text{ cm}^{-2}$. On the other hand, $H_{11}(2 \times 10^6 \text{ cm}^{-1})$ decreases by 8.5% for the same change in N_s . Therefore, it is concluded that the wave function is not too sensitive to temperature and inversion carrier density. These are fortunate results from the viewpoint of numerical simulations of electron devices with space-dependent carrier concentration. The scattering rate and subband coupling coefficients will need little or no updating during a simulation. Consequently, the tabulation of $H_{mn}(Q)$ (including the case of $m = n$), as shown in Fig. 2, will greatly reduce computational times without sacrifice of accuracy.

Financial support by the Army Research Office is gratefully acknowledged. One of the authors (K.Y.) thanks Professor S. Muroga for his encouragement and support during his stay at the University of Illinois.

¹See, for example, T. Ando, A. B. Fowler, and F. Stern, Rev. Mod. Phys. **54**, 437 (1982).

²F. Stern and W. E. Howard, Phys. Rev. **163**, 816 (1967).

³T. Ando, J. Phys. Soc. Jpn. **51**, 3893 (1982).

⁴K. Hess, Appl. Phys. Lett. **35**, 484 (1979).

⁵P. J. Price, Ann. Phys. (N. Y.) **133**, 217 (1981).

⁶P. J. Price, Surf. Sci. **113**, 199 (1982).

⁷P. J. Price, Phys. Rev. B **30**, 2234 (1984).

⁸L. Hedin and B. I. Lundqvist, J. Phys. C **4**, 2064 (1971).

⁹F. Stern, Phys. Rev. B **30**, 840 (1984).

¹⁰P. C. Chow, Am. J. Phys. **40**, 730 (1972).

¹¹In this approximation,

$$1/b_{mn} = 2 \int F_m(z) F_n(z) dz$$

and

$$C_{mn} = \frac{4b_{mn}}{\pi^2} \frac{m^2 + n^2}{(m^2 - n^2)^2}$$

were used. To get the approximate values of $H_{mn}(Q)$, the above defined b_{mn} and C_{mn} were used.

¹²The fractional occupations for the three lowest subbands were 0.9802, 0.0183, and 0.0014 at 77 K, and 0.6801, 0.1777, and 0.0771 at 300 K. The separations between the second and the third subband and above were of the same order of magnitude as the thermal energy at 300 K. The material parameters are the same as for Fig. 1.